PULSED MAGNETS FOR INJECTION AND EXTRACTION SECTIONS OF NSLS-II 3 GeV BOOSTER

A. Zhuravlev, A. Batrakov, A. Chernyakin, V. Kiselev, V. Konstantinov, A. Pavlenko,
V. Petrov, E. Semenov, D. Senkov, BINP, Novosibirsk, 630090, Russia

Abstract

Magnets for injection and extraction sections of NSLS-II 3 GeV booster are designed, manufactured and tested at BINP, Russia. This report considers the details of bump and septum magnets design, their parameters and results of the inspection test at BINP. The design and electronics features of the measurement stand for these magnets are presented. Also, capabilities of specialized power supplies are listed and discussed.

INTRODUCTION

NSLS-II is a new third-generation storage-ring light source that is under construction at Brookhaven National Laboratory. The booster NSLS-II will accelerate electrons from 200 MeV to the nominal energy of 3 GeV. The repetition rate of the booster is 1 or 2 Hz, depending on the state of the injector. In order to reduce the requirement for the linac's beam charge, the booster injection was designed to provide beam stacking [1, 2].

Pulsed magnets are used to realization the beam injection and extraction process. Table 1 shows the parameters of the pulsed magnets.

Table 1: Pulsed magnet parameters for booster injection and extraction scheme.

Parameter	Injection septum	Extraction septum	Bump Magnets
Energy, MeV	200	3000	3000
Effective Length, m	0.749	0.6	0.169
Field, T	0.111	0.8	0.46
HL, T*m	0.083	0.48	0.078
Angle, mrad	125	48	7.8
Magnetic gap, mm	30	16	33
Pulse duration, ½ sine μs	106	156	1500
Field error tolerance, %	±0.05	±0.02	±0.2
Stray field ∫H_{out}dl	≤ 1 Gs*m	≤ 1 Gs*m	-
Septum thickness, mm	4.2	4.2	-
Peak Current, A	2800	10220	1500
Peak Voltage, V	215	510	870
Self-inductance, μH	1.8	2.1	55
Power loss (2 Hz)W	10	150	20

SEPTUM MAGNETS

Figure 1: Top view of the injection septum magnet.

Eddy-current type septum magnets placed out of the vacuum chamber are used for the NSLS-II booster. The pulsed septum magnet consists of the C-shape laminated iron yoke with a single-turn excitation coil (Fig. 1.).
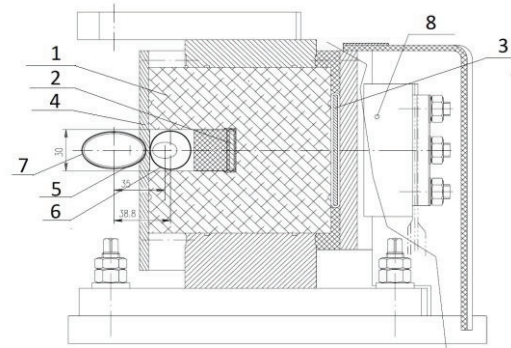

Figure 2: Cross-section view of the injection septum magnet.
1 – Laminated steel yoke, 2 – inner copper conductor, 3 – backleg winding, 4 – copper screen, 5 – iron screen, 6 – vacuum chamber of the magnet, 7 – vacuum chamber of the ring, 8 – current feedthrough.

The lamination of the iron yoke for the pulsed septum magnet is manufactured from cold rolled, oriented, low carbon steel - the thickness is 0.35 mm with ET coating (Fig. 2.). The coil and iron yoke are vacuum impregnated with the EPC-1 epoxy resin filled with aluminum. The magnet is connected with the power supply system by means of flat strips (8 in Fig. 2). Injection and extraction septums are similar in design and differ only in effective length, bending radius, field magnitude and aperture. The extraction septum magnet is equipped with indirect water cooling of the yoke.

All magnets (two septums and four bump magnets) are equipped with inductive coil, built in magnet, for the measurement of the magnetic field in the aperture.

A copper screen around the vacuum chamber limits penetration of the magnetic field into an equilibrium orbit. In order to significantly reduce the stray field the iron screen is additionally used. Effective thickness of the septum knife is 4.2 mm (see Fig. 3).
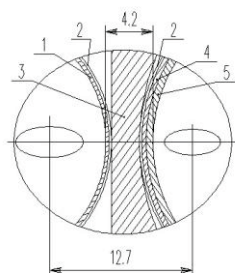

Figure 3: Cross-section view of the knife of the septum magnet.
1 – vacuum chamber (VC) of the magnet (0.3 mm),
2 – insulation (double layer 0.13 mm fiberglass tape),
3 – copper screen (2.5 mm),
4 – iron screen round the VC of the booster (0.4 mm),
5 – VC of the booster (0.8 mm).

Measurements of the field integrals were made with the matrixes consisting of 7 coils. The length of the matrix for the injection magnet is 900 mm (750 mm for extraction), bending radius is 6 m (12.5 for extraction), and the distance between the coils is 4 mm (2.2 mm for extraction). A fast precise digital integrator was developed to provide the accuracy of the measurements of the field parameters of the pulsed magnets. This device is intended for measurement of the field pulse with the duration ranging from 5 µs and provides a relative accuracy better than $5 \cdot 10^{-5}$ [3].

Influence of the vacuum chamber on field distribution in the injection septum magnet is shown in Fig. 4. The thickness of the vacuum chamber of the injection septum is 0.4 mm (0.3 mm for the extraction magnet).
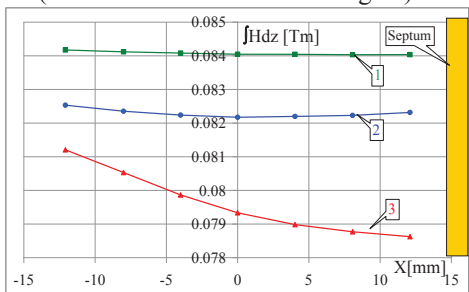

Figure 4: Distribution of the field integral in the aperture of the injection septum.
1 – Field distributional without vacuum chamber,
2 – Field distributional with vacuum chamber,
3 – The ends of vacuum chamber are short-circuited.

Placing of the vacuum chamber causes a weakening of the field amplitude by 2.2% for the injection septum and by 0.8% for the extraction septum. When vacuum chambers are short-circuited, additional 3.4% of field attenuation and nonlinearity occurs. To exclude such

effect the vacuum chamber of the magnet is insulated and its ends are provided with ceramic insertions.

Field distribution in different phases of the current pulse was measured. Position of the beam at the injection is X ≈ 5 mm (Fig. 5), beam size is $3\sigma_X \approx 4$ mm.
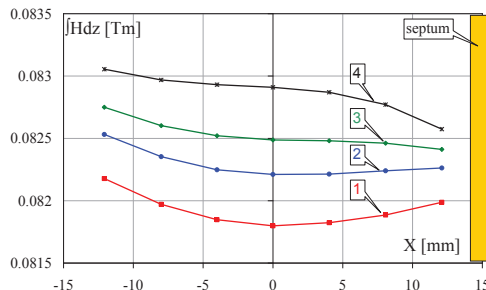

Figure 5: Inhomogeneity of the field integral in the magnet during various moments of time.
1 – t=52.5 µs, 2 – t=53.5 µs, 3 – t=54.5 µs, 4 – t=56.5 µs.

The behavior of the magnetic field outside the septum screen was also measured (Fig. 6, 7).
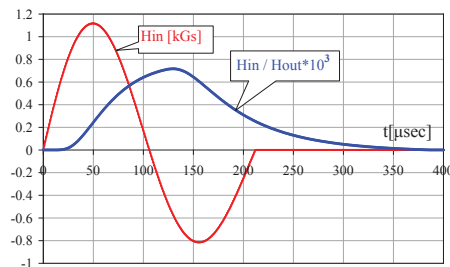

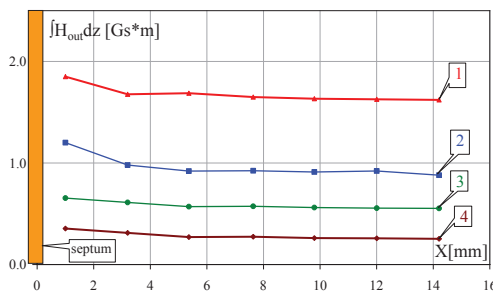Figure 6: The magnetic field in injection magnet and stray field in the vacuum chamber vs time.

Figure 7: Distribution of the stray field in the booster vacuum chamber at the various moments of time.
1 – Extraction septum t=75 µs (Hin = 0.8 T),
2, 3, 4 – Injection septum t=53 µs , t=106 µs, t=150 µs respectively.

We got a rather overstated value of the stray field caused by the fact that a 30-mm copper screen was not enough to suppress the field falling out of the magnet aperture.

BUMP MAGNETS

Four series-connected bumps shift the orbit from the center of aperture by 16 mm in the extraction section. "H"-shape bump magnet consists of the yoke and two coils (upper and lower). The yoke consists of two half-

cores (upper and lower). Each half-core is manufactured from a set of punched laminations (thickness - 0.5 mm) that are glued into a single block.

Figure 8: General view of the bump magnet.

Transverse distribution of bump magnetic field was measured with a long coil. Transverse position of the coil was changed by stepper motors. Fig. 8 shows the bump magnet with the measuring coil installed on a measurement stand. The duration of the feeding pulse of the bump magnets is 1.5 ms. Beam is in the phase of this pulse from 0 to 90 degrees. A thin-wall vacuum chamber (0.5 mm) is used to reduce the field attenuation and non-uniformity.
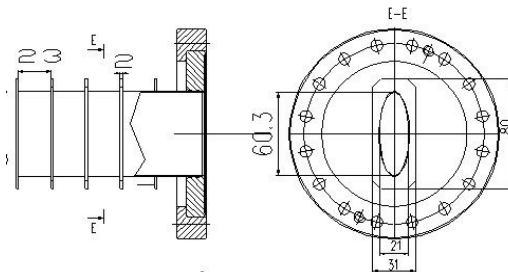

Figure 9: Vacuum chamber of the bump magnet.

The chamber looks like an ellipse with 10 x 30 mm semi-axes. Reinforcing ribs brazed to the chamber increase its mechanical strength. The ribs are 2 mm thick and spaced with a step of 23 mm (Fig. 9).

Integral of the field distribution in the bump magnet was measured in different phases of a feeding current pulse (Fig. 10).
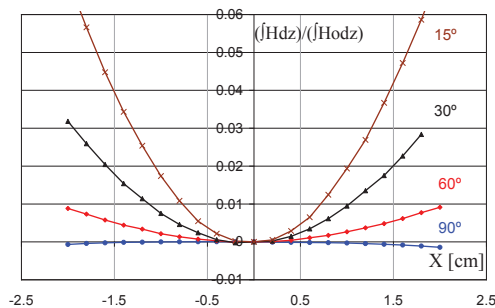

Figure 10: Inhomogeneity of the field integral in the bump magnet normalized on field integral in the centre for various phases of a current pulse.

According to the requirements for identity, the bump magnets should provide the spread of integrated fields of the magnets less than $d(HL)/HL \leq 2*10-3$. The measurements showed that the spread of integrated fields was more than that required (Fig. 11.).
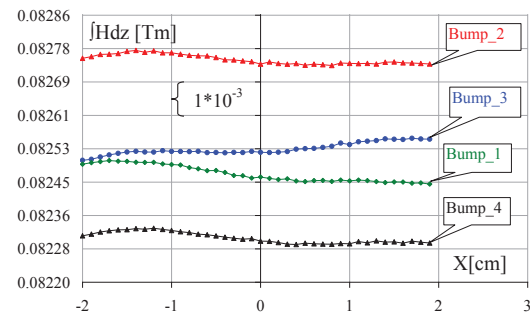

Figure 11: Integrated field value of the bump 1 ÷ bump 4 with the vacuum chamber.

The spread of the magnetic field at the level of 0.5% caused by the different arrangement of the individual flanges of the vacuum chambers relative to the bump magnets. According to the measurement results, the magnet with the lowest magnetic field was selected as a base. Then, for the remaining 3 bump magnets, a shunt with variable inductance was added to provide the spread of the field integrals not larger than $2*10^{-3}$ (Fig. 12).
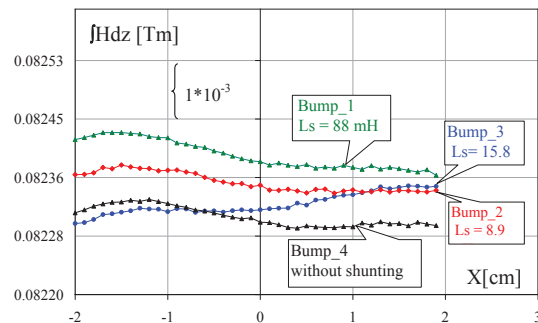

Figure12: Integrated field value of bump 1 ÷ bump 4 with the vacuum chamber and with shunting inductance.

CONCLUSION

All pulsed magnets have been completely constructed and assembled at the NSLS-II booster. Integrated tests were carried out and gave good results. The injection and extraction sections of the booster are ready for accelerator start-up. The authors would like to acknowledge the excellent work by our colleague from BINP S. Sinyatkin on initial modelling of the fields in the magnets. This work is supported by the Ministry of Education and Science of the Russian Federation.

REFERENCES

[1] T. Shaftan et al., «Status of the NSLS-II injection system», WEPEA082, Proceedings of IPAC'10, Kyoto, Japan.
[2] R. P. Fliller, R. Heese, S. Kowalski, J. Rose, T. Shaftan, G. Wang «Bean stacking in the NSLS-II », TUPEC041, Proceedings of IPAC'10, Kyoto, Japan.
[3] A. Batrakov, A. Pavlenko, I.Ilyin, «Electronics for precise measurements of accelerator pulsed», these proceedings, THPEA033.